

JOHN G. PARKER

OPTICAL MONITORING OF THE GENERATION OF SINGLET OXYGEN DURING PHOTODYNAMIC TREATMENT OF TUMORS

Research at APL has been directed at understanding energy transfer events taking place after laser excitation of photosensitive compounds in condensed media. In particular, optical means have been developed for the detection of electronically excited molecular oxygen (singlet oxygen) resulting from a favored energy transfer from the sensitizer triplet state. Oxygen excited in this manner is thought to play a key role in a new means for treating certain types of cancer. Recently at APL, small-animal experiments were conducted in which singlet oxygen generation was detected in laser-irradiated, presensitized, small-animal tumors.

INTRODUCTION

Photodynamic therapy, a relatively new treatment for cancer, has evolved from the investigational stage and is now being evaluated clinically under protocols approved by the U.S. Food and Drug Administration for certain types of cancer. Results obtained to date indicate that the treatment is promising, although it has some limitations.^{1,2} The therapy involves the cooperative action of an injectable tumor-specific sensitizer and light; the light is usually provided by the output of a laser. The general view, supported by a large body of *in vitro* data, is that the most important agent of tumor destruction is electronically excited oxygen (singlet oxygen) generated by a favored energy transfer from the optically excited sensitizer to ambient ground-state oxygen. Therefore, to understand the limitations of photodynamic therapy in cancer treatment, one must understand fully the nature of singlet oxygen interactions in the *in vivo* environment, which requires appropriate detection and measurement means.

Toward this end, measurements were made recently at APL in which emission accompanying singlet oxygen generation was detected during photodynamic treatment of murine (mouse) tumors.³ That demonstration represented the culmination of several years of research that focused on energy transfer processes involved in the photosensitized production of singlet oxygen in condensed media. Part of the earlier research was described in two articles that appeared in previous issues of the *Johns Hopkins APL Technical Digest*.^{4,5}

THE PHOTODYNAMIC PROCESS

The photodynamic process we are studying is one in which light is absorbed by a suitable dye molecule, lead-

ing to an excited state of the dye. The energy is transferred subsequently to ambient molecular oxygen, leading to the formation of an electronically excited state of this electrically neutral species. The spectral designation of this excited singlet molecular state is $O_2(^1\Delta_g)$, in contrast to the ground triplet state $O_2(^3\Sigma_g^-)$. (In this article, $O_2(^1\Delta_g)$ shall be designated as 1O_2 , and $O_2(^3\Sigma_g^-)$ shall be designated as 3O_2 .) The distinguishing feature of 1O_2 is that it reacts chemically with substances toward which 3O_2 is totally inert. Most importantly, such substances are known to constitute critical components of bacterial and mammalian cells.

Not all interactions of 1O_2 at the molecular level lead to a chemical or biochemical reaction. In a significantly large number of cases, the oxygen molecule simply returns to the ground state, and the excess energy is liberated as heat; that is, a physical deactivation occurs. Interpreted in a strict sense, the term "photodynamic process" is restricted to those cases in which a chemical reaction occurs.⁶

A very important property of ground-state molecular oxygen is that it exists in a triplet state, meaning that two electrons have their spins aligned in parallel. This condition creates a net magnetic moment, which is responsible for the paramagnetic properties of the molecule. An overwhelming majority of stable molecules in the ground state exist in a singlet state in which all electron spins are paired; that is, for every electron in a given quantum state, another electron has its spin oriented in the opposite direction, leading to a zero magnetic moment for the molecule as a whole. Absorption of an incident photon will raise the singlet dye molecule to a higher electronic energy, but no net change in spin con-

figuration will occur. Thus, the excited state remains a singlet.

In certain molecules, however, intramolecular coupling forces may cause a conversion from the excited singlet state to a triplet state of lower energy in which the molecule possesses a net electron spin. The triplet state is substantially elevated above the ground state, although it is less energetic than the excited state. Transformation of the triplet state back to the ground singlet is a very inefficient process because of problems associated with spin conservation; thus, this state of the dye molecule has a relatively long lifetime. In the presence of ground-state triplet oxygen, however, an intermolecular spin-conserving and energetically favorable interaction occurs in which the dye molecule returns to its ground state while the oxygen is simultaneously raised to its first excited singlet $^1\text{O}_2$ state (triplet + triplet \rightarrow singlet + singlet). The energy of the $^1\text{O}_2$ state is about 1 eV; if this energy were higher by a factor of 2 or 3, it could well exceed the energy available in the sensitizer triplet state, thus rendering the exchange impossible.

Having thus produced the required $^1\text{O}_2$, a quantitative method must be found to determine the amounts generated. In the past, investigators have used indirect methods involving the addition of substances (chemical acceptors or traps) that selectively undergo bleaching or other property changes. Those methods, however, have been used primarily in carrying out *in vitro* cell studies.^{7,8} For the *in vivo* case, the usefulness of chemical acceptors or traps is severely limited by problems associated with their solubility in a heterogeneous environment, depletion, interactions with the excited sensitizer, and lack of accessibility.

SINGLET OXYGEN EMISSION IN CONDENSED MEDIA

An important property of $^1\text{O}_2$ is that it will, with small probability, undergo a collisionally induced transition to the ground state in which the associated energy is released radiatively. The resulting emission appears in a fairly narrow band (18-nm full width at half maximum [FWHM]) centered in the near infrared (IR) at a wavelength of 1270 ± 2 nm, depending on the solvent. Thus, for a nonpolar environment such as that characterizing lipids, the central emission wavelength is approximately 1272 nm, whereas for a highly polar environment such as H_2O , the wavelength shifts slightly, to 1268 nm. Fortunately, the shift is small in comparison with the width of the emission itself, thereby minimizing problems involved in a precise location of the emission band in heterogeneous media such as human tissue.

As mentioned previously, the $^1\text{O}_2$ emission is collisionally induced. Thus, higher collision rates correspond to greater emission intensities. Experimental investigation of the dependence of radiative lifetime on collision rate indicates a radiative lifetime of approximately 60 min for the isolated molecule, and half that value for the same molecule in air at 1 atm.⁹ In liquids, collision rates are high because of the extremely short mean free paths; therefore, the radiative lifetime should be reduced

by several orders of magnitude, and experimental data support this expectation. Furthermore, the radiative lifetime is roughly constant at 4 s for a wide variety of solvents ranging from H_2O , in which the decay time for physical quenching is 3 μs , to CCl_4 , in which the corresponding value is 30,000 μs .¹⁰

CLINICAL ASPECTS OF PHOTODYNAMIC THERAPY

The preceding discussion suggests that photodynamic therapy should be considered as a three-component system involving (1) a suitable injectable sensitizer, (2) a light-delivery system; and (3) a means for monitoring the production of $^1\text{O}_2$ produced through the combined effects of (1) and (2). Not only is it important to have a means of monitoring the $^1\text{O}_2$ levels instantaneously, but it is also essential that the means be used to establish dosimetry standards.

Previous clinical results have shown that dosimetry based on a measurement of incident light intensity alone is not a reliable indicator of treatment effectiveness. Thus, different patients receiving exactly the same amount of injected sensitizer per unit of body weight and the same light dosage may exhibit totally different reactions ranging from complete response to no response. Use of the word "response" in this connotation applies to the immediate post-therapy result and has no direct implication regarding long-term cure. Even more puzzling than the wide range of initial reactions are the significantly different responses that the same person may exhibit during successive treatments.

Measurements of intratissue sensitizer concentration and light intensity indicate that the two quantities may be predicted with reasonable accuracy from a knowledge of the injected sensitizer dose and incident light intensity. Variations observed clinically are, thus, probably due in one way or another to a deficiency in $^1\text{O}_2$ production. If the sensitizer concentration and incident light intensity are known, then one should be able to determine the levels of the sensitizer triplet states accurately. Transfer of this energy to form $^1\text{O}_2$ may be impeded for several reasons: (1) oxygen is initially available but is not replenished at a sufficient rate; (2) oxygen is available but in an environment characterized by slow diffusion rates, leading to a reduction in the rate of interaction with the triplet, which is quenched by other means; (3) the sensitizer is not located near vulnerable biological targets, so $^1\text{O}_2$ is generated but attacks only noncritical cell components; (4) certain cell components, such as beta carotene and alpha tocopherol, exert a protective effect by quenching either the sensitizer triplet or $^1\text{O}_2$; and (5) the sensitizer triplet lifetime depends on the local biological environment.

The foregoing list of possible difficulties involved in the production of $^1\text{O}_2$ through energy transfer from the sensitizer triplet state is by no means complete and is presented only to stress the complexity of the physiological environment. Obviously, one of the more important problems is that of oxygen depletion, which may occur because of relatively slow oxygen diffusion rates

or inadequate blood flow. The effect of restricting the blood flow in mice was shown to interfere with photodynamic effects.¹¹ Furthermore, the photodynamic effect itself was shown to reduce blood flow to tumors.¹²

Thus, a determination of $^1\text{O}_2$ production levels is mandatory if one is to employ the photodynamic process efficiently. A high $^1\text{O}_2$ concentration may be produced initially, but within a short time period, it may drop to a much lower steady-state level. In such a case, it would be far better to program the incident radiation in an on-off sequence designed to optimize the average $^1\text{O}_2$ level. Doing so, of course, would require a means to monitor this quantity to provide the necessary control.

DETECTION OF PHOTOSENSITIZED PRODUCTION OF $^1\text{O}_2$

Basic Concept

The $^1\text{O}_2$ emission at 1270 nm has been detected optically through the use of various detectors. Experimental measurements taken from 1200 to 1300 nm by using pulsed laser irradiation of various photosensitizers (primarily porphyrins) in different solvents have indicated the presence of an IR component of the sensitizer fluorescence.¹³⁻¹⁵ Although the fluorescence is quite weak in comparison with the primary visible emission, under the conditions of the high sensitivity required to detect the $^1\text{O}_2$ emission for certain solvents (e.g., H_2O , D_2O), it may become the dominant factor in terms of amplitude.¹³

Both the $^1\text{O}_2$ emission and IR sensitizer fluorescence arise as a result of the optical excitation of the sensitizer and are thus inextricably intertwined. Even if a narrow-bandpass IR filter is used to isolate the spectrally discrete $^1\text{O}_2$ emission, a relatively large amount of the spectrally diffuse, IR sensitizer fluorescence will still be transmitted to the detector.

The solution to the problem of detecting singlet oxygen emission against the large coherent IR fluorescence background is provided by considering the dynamics of the situation. For example, if the excitation source is suddenly turned on, the fluorescence appears immediately. The transfer of energy from the sensitizer triplet state, leading to the formation of $^1\text{O}_2$, is collisional in nature, however. Thus, the energy transfer takes a certain characteristic time τ_1 , and attainment of the $^1\text{O}_2$ equilibrium is correspondingly delayed. Conversely, if the excitation is turned off, the fluorescence disappears immediately, whereas the singlet oxygen emission decays relatively slowly with a time constant τ_2 that depends on the surrounding medium, resulting in an additional delay. Thus, the distinguishing difference between the sensitizer fluorescence (and also tissue-related fluorescence) and the $^1\text{O}_2$ emission is that the latter is delayed in time relative to the former.

The experimental approach that was adopted involves chopping the excitation to generate a series of on-off light pulses and then comparing the phase of the resultant IR fluorescence plus $^1\text{O}_2$ emission with that of the fluorescence alone. Figure 1 shows the phase relationship between the delayed singlet oxygen emission **B** and

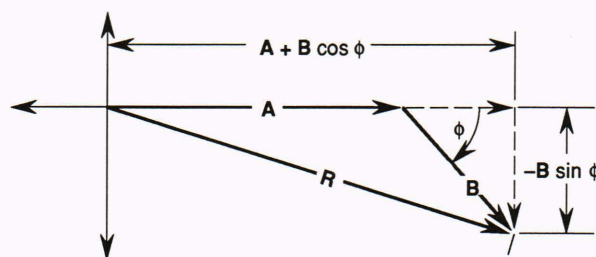


Figure 1. Phase relationship of the IR sensitizer fluorescence **A** and the delayed singlet oxygen emission **B** following periodic optical excitation of the sensitizer. The resultant signal **R** contains a component in phase with **A** ($A + B \cos \phi$) and a quadrature component ($-B \sin \phi$), whose magnitude is independent of **A**.

the IR fluorescence **A**. The resultant signal **R** contains a component in phase with **A** and a component that lags by 90° , that is, the so-called quadrature component, whose magnitude is independent of **A**. Vector **A** must have a quadrature component of zero. This condition may be achieved readily by using a second bandpass filter that transmits totally outside the $^1\text{O}_2$ emission band. Thus, the establishment of a quadrature null for the fluorescence component and the subsequent determination of the $^1\text{O}_2$ quadrature reading require a two-wavelength optical comparator, which is an integral part of the optical input system preceding the detector.

The theoretical variation³ of the in-phase and quadrature components of the singlet oxygen emission is shown in Figure 2 for an air-saturated water sample characterized by a triplet energy transfer time $\tau_1 = 2.13 \mu\text{s}$ and a singlet oxygen decay time $\tau_2 = 3.20 \mu\text{s}$.¹⁶ The in-phase $^1\text{O}_2$ component (fluorescence left out) has its maximum at a low chopping frequency, declines to zero, becomes slightly negative, and then slowly approaches zero as the chopping frequency is increased. On the other hand, the negative quadrature component starts out at zero, slowly increases to a maximum value equal to about half the maximum in-phase value, and then slowly declines to zero at high chopping frequencies.

Thus, an optimum chopping frequency exists at which the quadrature signal is maximized. In the case of the air-saturated aqueous sample considered here (oxygen tension = 150 mm), the optimum frequency is about 34.5 kHz. For reduced oxygen tension, characterizing tissue interstitial fluid (40 mm¹⁷), the peak drops to 13 kHz. The optimum frequency is also lower for a completely lipid environment (5 kHz).

Instrumentation

The experimental system used in carrying out the measurements is shown schematically in Figure 3. The output of an argon ion laser is used to pump a dye laser operating with DCM* as the active dye. This setup provided an output wavelength in the range from 600 to 700 nm; the wavelength selection was accomplished through the use of a single-element birefringent plate.

*DCM denotes 4-dicyanomethylene-2-methyl-6-p-dimethylaminostyryl-4H-pyran.

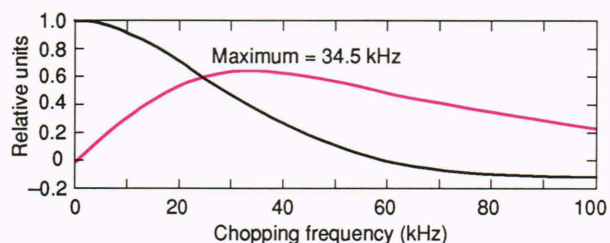


Figure 2. Frequency dependence of calculated values of the in-phase (black curve) and negative quadrature (red curve) components of singlet oxygen emission in an aqueous sample according to the theory presented in Ref. 3. The triplet energy transfer time $\tau_1 = 2.13 \mu\text{s}$, and the singlet oxygen decay time $\tau_2 = 3.20 \mu\text{s}$.

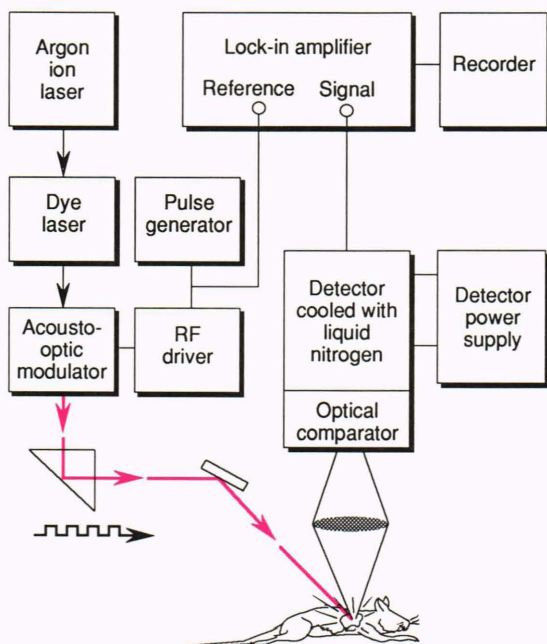


Figure 3. Block diagram of the apparatus used to detect $^1\text{O}_2$ emission from a laser-irradiated SMT-F tumor implanted subcutaneously in a DBA/2 mouse. Previously, the mouse had been injected intraperitoneally with Photofrin II at a level of 50 mg/kg. Incident laser power was typically 20 mW, and the wavelength was set at 630 nm. The hair covering the tumor was removed chemically. (Reprinted, with permission, from Ref. 3, p. 15, ©1987 IEEE.)

For most measurements, the wavelength was fixed at $630 \pm 1 \text{ nm}$ (measurements have indicated maximum biological effectiveness at this wavelength).¹⁸ The dye laser output was modulated by an acousto-optic modulator actuated by an RF driver. Modulation input to the driver was supplied in the form of a square wave from a synthesizer/function generator. The RF input to the acousto-optic modulator was monitored by a wattmeter.

The square-wave (equal on and off times) optical output emerging from the acoustic-optic modulator was then directed to the target by either a prism-mirror combination, as shown in Figure 3, or by a quartz fiber. A tumor that was implanted subcutaneously in a laboratory mouse is shown as the objective in Figure 3.

In all cases, the optical light collection system consisted simply of a 2.54-cm-diameter lens with a focal length of 25 mm that was used to direct the light emitted from the irradiated target through the optical filtering system and then into the germanium detector, which was cooled with liquid nitrogen. The detector time constant was determined to be $30 \mu\text{s}$, and the noise equivalent power was approximately 10^{-14} W in a 1-Hz bandwidth.

Optical input to the detector was filtered by using either the two-wavelength optical comparator indicated in Figure 3 or, alternatively, a spectrometer equipped with a grating blazed at $1 \mu\text{m}$. For all *in vivo* measurements, the spectrometer slit widths were 5 mm. The two-wavelength comparator was developed to improve the efficiency of optical coupling of the detector to the laser-irradiated objective. Improved coupling was needed because insertion of the spectrometer caused a signal loss of approximately 1 order of magnitude. Basically, the comparator is a two-wavelength spectrometer comprising two filters arranged mechanically in a sliding device. One of the filters (A) exhibits maximum transmission at 1215 nm with a width of 23 nm (FWHM), therefore lying completely outside the $^1\text{O}_2$ emission band; the other (B) is centered at 1282 nm with a width of 29 nm that significantly overlaps the region of $^1\text{O}_2$ emission, but exhibits negligible overlap with filter A. Because the signal obtained by using filter A contains essentially no component of the $^1\text{O}_2$ emission, only the sensitizer IR fluorescence is involved. Therefore, the signal is useful in establishing a reference (i.e., zero-phase condition) against which the quadrature component of the signal generated by light passing through filter B may be obtained.

An equivalent means was used for extracting the $^1\text{O}_2$ emission from the background produced by the sensitizer IR fluorescence when the spectrometer was employed. That method involved setting the spectrometer wavelength to 1200 nm and then adjusting the lock-in phase so as to produce zero quadrature component. With a slit width of 5 nm, the instrumental resolution was approximately 40 nm (FWHM), and essentially no overlap with the singlet oxygen emission occurred. Thus, the signal appearing at the lock-in input was composed entirely of the sensitizer fluorescence and, as such, provided a valid reference.

Resolution of the total detector output signal into the in-phase and quadrature components was achieved by means of a lock-in amplifier equipped with a preamplifier. The lock-in output was documented with a recorder.

BIOLOGICAL MEASUREMENTS

In vivo measurements of $^1\text{O}_2$ emission were carried out by using DBA/2 mice implanted subcutaneously with SMT-F tumors, and C3H mice implanted subcutaneously with RIF tumors (the mouse and tumor designations indicate the strain). In all cases, the mice were injected with a Photofrin II sensitizer at a level of 50 mg/kg of body weight. The time delay between injection and irradiation was 24 hours. The laser excitation wavelength was set at 630 nm in all cases.

Data presented in Figure 4 provide a comparison of $^1\text{O}_2$ emission levels in a medium simulating a biological environment with that obtained from an actual tumor. In obtaining the data, the chopping frequency was fixed at 20 kHz, and the incident intensity was approximately 25 mW. The four strip-chart recordings shown in the top of Figure 4 are the results obtained when a piece of porphyrin-impregnated beefsteak was used as a means of simulation. Each recording corresponds to a different location on the surface of the meat sample. The sample was cubical, with an edge approximately 1 cm long, and was immersed in a solution containing 1×10^{-4} molar hematoporphyrin in H_2O at a pH of 7.2 for five hours. Before irradiation with the laser, the sample was carefully rinsed with distilled water and then exposed to the output of a short-wavelength violet lamp. The resulting red fluorescence confirmed substantial porphyrin uptake.

Traces of the simulation data on the left side of Figure 4 indicate quadrature levels obtained after inserting the fluorescence-only filter centered at 1215 nm. Their averages are to be compared with those appearing on

the right side that were obtained by using the filter encompassing singlet oxygen emission, which was centered at 1282 nm. The important quantity is the numerical difference in levels in each case, the values of which appear in the center. As Figure 4 shows, the difference values of the four simulation spectra vary substantially, although they all significantly exceed the existing noise levels.

The bottom of Figure 4 shows similar results obtained for an RIF tumor implanted in a C3H mouse. The difference between the right and left sides is about $10 \mu\text{V}$, which compares favorably with the maximum obtained from the simulation. In general, the differences recorded for this type of tumor are comparable with those obtained from the simulation.

As discussed earlier, in validating the experimental method, spectral data are extremely important in establishing whether or not the detection system is unequivocally capable of singlet oxygen detection. Such a determination is even more important for the *in vivo* case because the biological medium is extremely complex and not at all homogeneous, with interfaces separating aqueous and lipid regions. Since the maximum $^1\text{O}_2$ emission levels observed were on the order of $10 \mu\text{V}$, and since insertion of the spectrometer into the system would introduce a loss of approximately 1 order of magnitude, small signals were expected. This result was obtained experimentally, as Figure 5 shows.

The data were obtained by using a DBA/2 mouse implanted with an SMT-F tumor. The Photofrin II injection level was 50 mg/kg, and irradiation occurred 24 hours post-injection at a level of approximately 20 mW. The excitation wavelength was 630 nm. Although the data are quite noisy, the expected increase in signal level of about $1 \mu\text{V}$ in the proximity of 1270 nm is quite

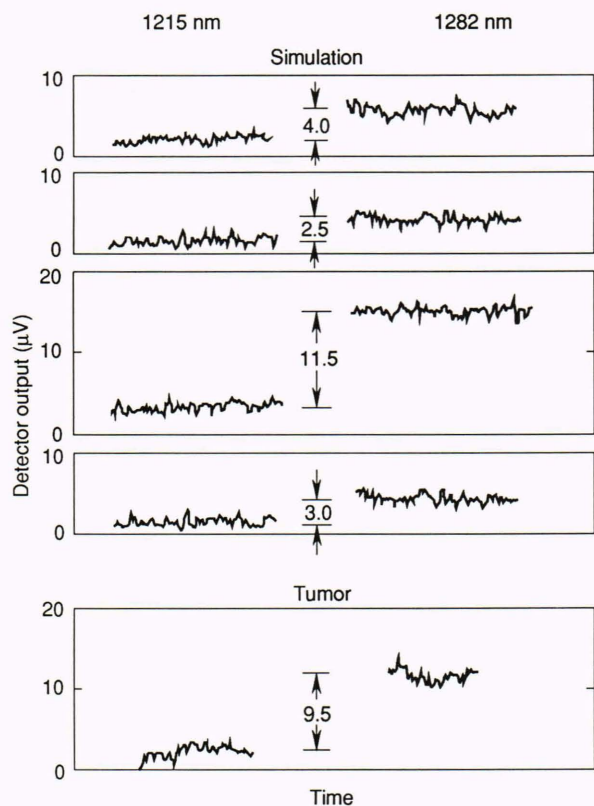


Figure 4. Comparison of experimental data obtained through simulation (top) with data obtained for an RIF tumor implanted in a C3H mouse (bottom). A two-band optical comparator was used to separate IR fluorescence from singlet oxygen emission. The fluorescence-only filter was centered at 1215 nm, and the filter encompassing singlet oxygen emission was centered at 1282 nm. The values in the center are the differences between the output at 1215 nm and the output at 1282 nm. The top four recordings correspond to four different locations on the surface of the meat sample used for the simulation.

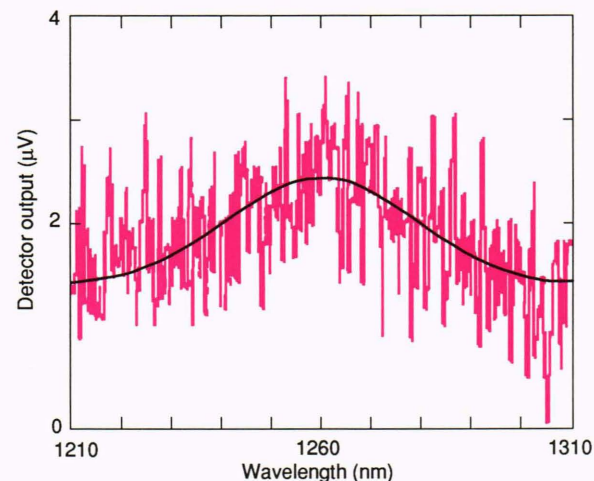


Figure 5. Spectral variation of the negative quadrature component obtained from a laser-irradiated, presensitized, SMT-F murine tumor. The black curve represents a computer-generated least-squares fit of the known spectral variation of $^1\text{O}_2$ emission with spectrometer slit widths set at 5 mm. The vertical displacement of the data is caused by instrumental offset. An intraperitoneal injection was given 24 hours before radiation at a level of 50 mg/kg. (Reprinted, with permission, from Ref. 3, p. 19, ©1987 IEEE.)

evident. The black curve represents a computer-generated least-squares fit to the data using the known spectral dependence for a spectrometer slit width of 5 nm.

In addition to the negative quadrature component, the in-phase component was also recorded. Those data appear in Figure 6A. From the data, we note the rather high levels of IR fluorescence, ranging from 300 μV at 1200 nm to approximately 150 μV at 1320 nm. As we shall see shortly, the high levels are due primarily to the sensitizer. Thus, for the *in vivo* case, the IR fluorescence level exceeds the $^1\text{O}_2$ emission intensity by more than 2 orders of magnitude.

Figure 6B shows a recording of the fluorescence measured from another mouse in which a similar tumor had been implanted but which had not been injected with the sensitizer. That recording, therefore, is the autofluorescence, which ranges from approximately 40 μV at 1200 nm to 15 μV at 1320 nm. Thus, the autofluorescence in that mouse is approximately 1 order of magnitude smaller than the sensitizer-generated IR fluorescence in the first mouse.

SUMMARY

In summary, it is possible to detect the intratumor generation of $^1\text{O}_2$ accompanying photodynamic treatment. The signals are modest, but the reported results represent a first attempt at using a system that was not optimized. Maximization of the overall system sensitivity is the next step, followed by a series of small-animal experiments, the objective of which will be to correlate the measured singlet oxygen dose with the effectiveness of the treatment.

REFERENCES

- Prout, G. R., Lin, C.-W., Benson, R., Nseyo, U. O., Daly, J. J., et al., "Photodynamic Therapy with Hematoporphyrin Derivative in the Treatment of Superficial Transitional Cell Carcinoma of the Bladder," *New England J. Med.* **317**, 1251-1255 (1987).
- Edell, E. S., and Cortese, D. A., "Bronchoscopic Phototherapy with Hematoporphyrin Derivative for Treatment of Localized Bronchogenic Carcinoma: A Five-Year Experience," *Mayo Clin. Proc.* **62**, 8-14 (1987).
- Parker, J. G., "Optical Monitoring of Singlet Oxygen Generation During Photodynamic Treatment of Tumors," *IEEE Circuits Devices Mag.* **3**, 10-21 (1987).
- Parker, J. G., and Stanbro, W. D., "Energy Transfer Processes Accompanying Laser Excitation of Hematoporphyrin in Various Solvents," *Johns Hopkins APL Tech. Dig.* **2**, 196-199 (1981).
- Parker, J. G., "The Importance of Singlet Delta Oxygen in Cancer Photoradiation Therapy," *Johns Hopkins APL Tech. Dig.* **5**, 48-50 (1984).
- Blum, H. F., *Photodynamic Action and Diseases Caused by Light*, Reinhold, New York (1941).
- Weishaupt, K. R., Gomer, C. J., and Dougherty, T. J., "Identification of Singlet Oxygen as the Cytotoxic Agent in Photo-inactivation of a Murine Tumor," *Cancer Res.* **36**, 2326-2329 (1976).
- Moan, J., and Sommer, S., "Oxygen Dependence of the Photosensitizing Effect of Hematoporphyrin Derivative in NHIK 3025 Cells," *Cancer Res.* **45**, 1608-1610 (1985).
- Badger, R. M., Wright, A. C., and Whitlock, R. F., "Absolute Intensities of the Discrete and Continuous Absorption Bands of Oxygen Gas at 1.26 and 1.065 and the Radiative Lifetime of the $^1\Delta_g$ State of Oxygen," *J. Chem. Phys.* **43**, 4345-4350 (1965).
- Krasnovsky, A. A., Jr., "Quantum Yield of Photosensitized Luminescence and Radiative Lifetime of Singlet ($^1\Delta_g$) Molecular Oxygen in Solution," *Chem. Phys. Lett.* **81**, 443-445 (1981).
- Gomer, C. J., and Razum, N. J., "Acute Skin Response in Albino Mice Following Porphyrin Photosensitization Under Oxidic and Anoxic Conditions," *Photochem. Photobiol.* **40**, 435-439 (1984).
- Selman, S. H., Kreimer-Birnbaum, M., Klaunig, J. E., Goldblatt, P. J., Keck, R. W., et al., "Blood Flow in Transplantable Bladder Tumors Treat-

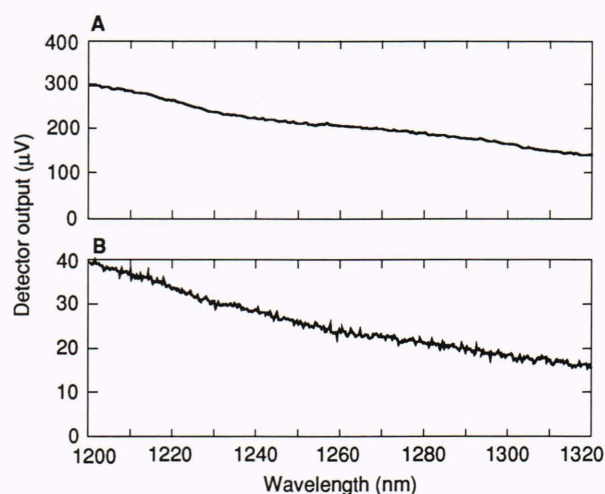
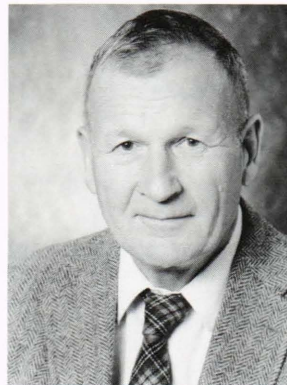


Figure 6. Fluorescence recordings. **A.** Spectral variation of the in-phase component of the detector response to emission from the murine tumor described in Figure 5. **B.** Spectral variation of the in-phase component of the detector response to emission from a similar tumor implanted in a second mouse that had not been injected previously. (Reprinted, with permission, from Ref. 3, p. 19, ©1987 IEEE.)

ed with Hematoporphyrin Derivative and Light," *Cancer Res.* **44**, 1924-1927 (1984).

- Parker, J. G., and Stanbro, W. D., "Dependence of Photosensitized Singlet Oxygen Production on Porphyrin Structure and Solvent," in *Porphyrin Localization and Treatment of Tumors*, Doiron, D. R., and Gomer, C. J., eds., Alan R. Liss, New York, pp. 259-284 (1984).
- Krasnovsky, A. A., Jr., "Photosensitized Luminescence of Singlet Oxygen in Aqueous Solutions," *Biophysics Engl. Transl.* **24**, 769-771 (1980).
- Krasnovsky, A. A., Jr., "Luminescence of Singlet State Oxygen in Solutions of Photosensitizers," *J. Appl. Spectrosc. Engl. Transl.* **32**, 492-496 (1980).
- Parker, J. G., and Stanbro, W. D., "Optical Determination of the Rates of Formation and Decay of $\text{O}_2(^1\Delta_g)$ in H_2O , D_2O , and Other Solvents," *J. Photochem.* **25**, 545-547 (1984).
- Guyton, A. G., "Transport of Oxygen and Carbon Dioxide in the Blood and Body Fluids," Chap. 41, in *Textbook of Medical Physiology*, 6th Ed., W. B. Saunders Co., Philadelphia, pp. 504-515 (1981).
- Gomer, G. J., Doiron, D. R., Rucker, N., Razum, N. J., and Fountain, S. W., "Action Spectrum (620-640 nm) for Hematoporphyrin Derivative Induced Cell Killing," *Photochem. Photobiol.* **39**, 365-368 (1984).

THE AUTHOR



JOHN G. PARKER received an Sc.B. in electrical engineering (cum laude) from Brown University in 1947. He later received an Sc.M. in physics (1950), followed by a Ph.D. in physics (1952), also from Brown University. After a brief stay at The Johns Hopkins University Institute for Cooperative Research, Dr. Parker joined the Sound Division of the Naval Research Laboratory. In 1956, he joined the Milton S. Eisenhower Research Center at APL, and he was appointed to APL's Principal Professional Staff in 1966. At APL, Dr. Parker has conducted both experimental and theoretical research

on molecular energy transfer processes in gases and condensed media. Most recently, his research has involved the study of laser-induced processes in biological media.